Technical Paper
BR-1876

Corrosion in Alloy Wet FGD Absorber Reaction Tanks

Authors:
P. Bonnin-Nartker
S.R. Brown
R.F. DeVault
J.M. Jevec
M.G. Milobowski
K.J. Rogers
J.M. Sarver
S.P. Ulbricht

Babcock & Wilcox
Power Generation Group, Inc.
Barberton, Ohio, U.S.A.

Presented to:
Power Plant Air Pollutant Control "MEGA" Symposium

Date:
August 20-23, 2012

Location:
Baltimore, Maryland, U.S.A.

babcock & wilcox power generation group

Corrosion in Alloy Wet FGD Absorber Reaction Tanks

P. Bonnin-Nartker
S.R. Brown
R.F. DeVault
J.M. Jevec
Babcock & Wilcox Power Generation Group, Inc.
Barberton, Ohio, USA

M.G. Milobowski
K.J. Rogers
J.M. Sarver
S.P. Ulbricht
Babcock & Wilcox Power Generation Group, Inc.
Barberton, Ohio, USA

Presented at:
Power Plant Air Pollutant Control "MEGA" Symposium
Baltimore, Maryland, U.S.A.
August 20-23, 2012

BR-1876

Abstract

Unexpected aggressive corrosion has been observed in alloy wet flue gas desulfurization (FGD) absorber reaction tanks industry-wide. Babcock & Wilcox Power Generation Group, Inc. (B&W PGG) has conducted research on the potential causes of this corrosion, associated process chemistry implications, and development of a test methodology to assess suitability of materials in the wet FGD environment. A primary cause of corrosion appears to be fluoride-induced under-deposit attack. Additionally, highly oxidative environments within some absorbers cause manganese in the slurry to precipitate as manganese oxide, thereby creating a galvanic effect which appears to greatly exacerbate the under-deposit attack mechanism. Various process chemistry parameters that influence manganese deposition also have implications on mercury, selenium and other trace metal phase partitioning, and on acid gas emissions. Presented in this paper are analytical data and results from various process slurries and deposits from operating units, and laboratory data from tests that recreate the observed reaction tank corrosion and predict the behavior of candidate alloys.

Introduction

In May 2009, after eleven months of operation by a midwestern utility, an unexpected aggressive level of corrosion was discovered on the interior walls and floor of a forced oxidation, limestone reagent B&W PGG absorber reaction tank fabricated from 2205 duplex stainless steel (UNS S32205). Similar corrosion was later observed in September 2009 in this plant's sister absorber reaction tank. In general, this severe corrosion occurred over the entire absorber reaction tank surfaces below the liquid level, particularly on the lower shell courses and in low-velocity areas. Both plate and heat-affected zone (HAZ) surfaces were affected; however, no corrosion of the Alloy 625 (UNS N06625) weld filler metal was observed (refer to Figure 1). Although this degree of severe corrosion has not been observed in any other B&W PGG reaction tanks, it has been reported by other utilities in competing suppliers' jet bubbling reactors and spray tower reaction tanks fabricated from Alloy 2205, and to a significantly lesser degree in reaction tanks fabricated from austenitic stainless steel and 6% molybdenum stainless.

Due to concerns about the unexpected corrosion of 2205 duplex stainless steel absorber reaction tanks, utilities have increased their inspections of such tanks. For those reaction tanks not showing any indications of the aggressive corrosion, some observations of a less severe surface etching and sub-surface pitting mechanism have been discovered (refer to Figure 2).

Fig. 1 Aggressive corrosion near vertical weld.

Fig. 2 Less severe surface etching.

Neither the aggressive corrosion, nor the less severe surface etching and sub-surface pitting corrosion, has been reported on any 2205 duplex stainless steel absorber tray tower surfaces above the flue gas inlet. Though corrosion has been observed in slurry spray alloy headers, such corrosion is considered to be caused by the same attack mechanisms as the wetted surfaces of the absorber reaction tank.

This paper will summarize three years of research by B&W PGG into these corrosion problems.

Discussion

Reaction Tank – Aggressive Corrosion

A joint root cause investigation of the unexpected aggressive corrosion in the two absorber reaction tanks was undertaken by B&W PGG, the utility, and the utility's consulting firm. The investigation focused on three primary areas as potential root causes: (1) base alloy and weld material issues, (2) welding process and fabrication issues, and (3) corrosive environment. After a lengthy and rigorous investigation, no evidence was found that material selection, weld process, or fabrication deficiencies were responsible for the level of corrosion observed. The presence of this degree of corrosion in the midwestern utility's two absorber reaction tanks, but not in those of other B&W PGG-supplied Alloy 2205 absorbers, indicated that the corrosion process is the result of highly corrosive process chemistry.

The aggressive corrosion sites observed in the absorber reaction tanks were covered by scale, but not all areas covered by scale exhibited visible corrosion. Corrosion varied from small pits to through-wall penetration of the shell. Numerous scale samples were collected from corrosion-covered areas during the May 2009 outage, and analyzed. Samples varied in visual characteristics, and were generally grouped by color: black, green, and rust/brown. The samples of hard, black scale were found to be rich in manganese and fluorine. The major elements in the dark green scale were fluorine and chromium. One hypothesis is that when fluoride, which is extremely corrosive when present in a concentrated wetted form, attacks the Alloy 2205, chromium is released into the scale as a corrosion product. The rust-colored/brown scale was found to be rich in fluorine, chromium and iron; chromium and iron being corrosion products of Alloy 2205.

Laboratory Immersion Testing

As part of the investigation, Alloy 2205 weld zone and base metal coupons were exposed to pH-adjusted absorber slurry liquor solutions for 44 days at approximately 132°F (55.5°C). The weld zone coupons contained weld, HAZ, and base metal; the base metal coupons were not subjected to any welding. The liquors used in this testing were taken from operating units' samples collected in June, 2009; some liquors were taken from reaction tanks exhibiting severe corrosion, and some from tanks that were not. Prior to testing, the solids were filtered from the liquors, and the pH was adjusted by the addition of sulfuric acid to match that of the reaction tank environment; the liquors were not chemically modified in any other way. The pH of the liquor from the unit showing the unexpected aggressive corrosion was adjusted from 6.85 to 5.37. The pH of the liquor from the non-corroding Control unit was adjusted from 6.71 to 5.36. The test flasks were continuously sparged with air to simulate the effect of oxidation air in the absorber reaction tank.

From the results of the immersion testing, the authors conclude that the liquor from the aggressively corroded reaction tank caused corrosion not only to the area of welds and HAZ, but also to the base metal unaffected by welding (refer to Figure 3). Consistent with electrochemical testing done on absorber slurry liquor after filtering from eight plants, the liquor from the aggressively corroding reaction tanks showed a greater than 2.0 unit reduction in pH from the start to the end of the 44-day immersion test (refer to Figure 4), whereas the Control liquor experienced a 0.5 unit increase in pH.

Additional sampling and analyses were conducted on slurry and process water stream samples taken from eight wet FGD units. While standard analyses did not yield any obvious differences between the scrubber solutions that could be

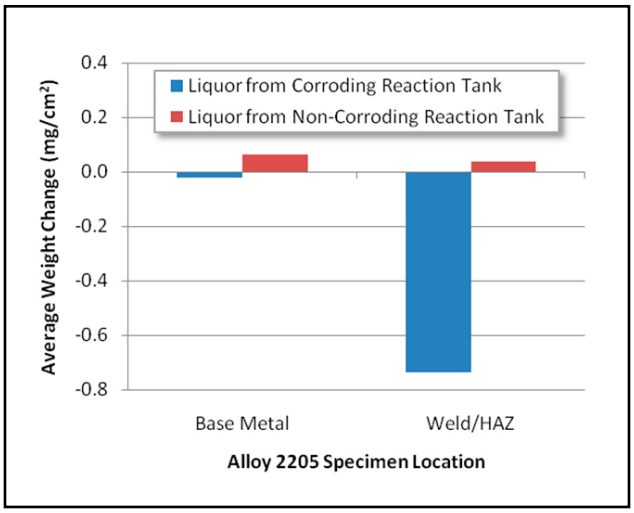

Fig. 3 Change in corrosion after 44-day immersion.

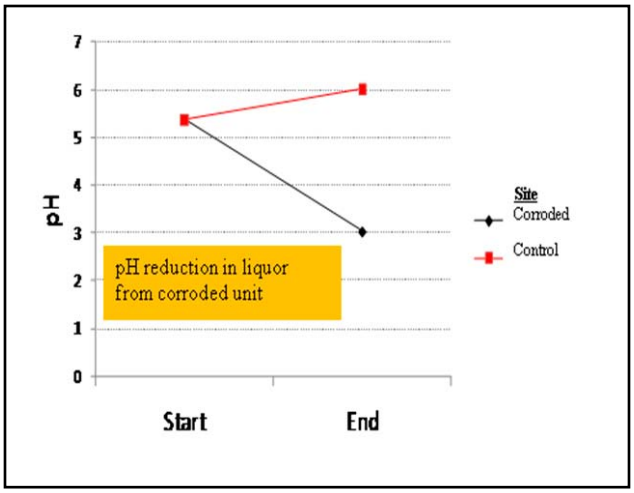

Fig. 4 Change in pH of absorber slurry filtrate after 44-day immersion.

defined as the root cause of the aggressive corrosion, phase partitioning of manganese (Mn) was evident (refer to Table 1). According to Lutey and Richardson, manganese, when precipitated as an oxide, is an enobling compound that raises the pitting tendency of the alloy.[1] Manganese in solution is not a corrosion concern. Note that the oxidation reduction potential (ORP) of the absorber slurry was below 400 mV for the non-corroding units, compared to ORP values significantly greater (factors ranging from 2 to 3) than 400 mV for the corroding units. ORP, also known as the Redox potential, is a voltage measure against reference electrodes of the net strength of oxidizers and reducers in a solution.

Another observation was that spontaneous precipitation occurred in filtrates from units experiencing aggressive corrosion. The precipitate continues to form even after multiple filterings, which suggests it is not related to solubility.

Table 1
Composition of Precipitated Solids Filtered from Absorber Slurry Filtrate of Operating Units, Wt. %, as Obtained by SEM/EDS

	Corrosion		No Corrosion			
O	47.83	47.72	55.14	54.63	52.80	67.47
F	1.89	1.17	0.59	1.62	2.72	2.41
Na	<0.01	<0.01	0.35	2.04	<0.01	0.34
Mg	6.02	6.05	18.86	10.37	0.67	6.80
Al	3.75	3.72	0.20	1.45	13.60	1.81
Si	1.31	1.20	0.93	2.87	21.77	3.19
S	5.45	6.03	21.68	7.45	0.52	3.68
Cl	3.10	3.19	0.24	12.61	1.54	8.66
K	0.26	0.17	0.07	0.78	0.20	0.55
Ca	2.31	2.71	1.23	3.00	5.09	1.82
Mn	23.34	23.78	0.06	0.31	0.09	0.27
Fe	0.83	0.73	0.10	1.30	0.23	0.87
Ni	0.53	0.50	0.10	0.36	0.25	0.46
Cu	0.61	0.59	0.24	0.69	0.32	1.06
Zn	2.13	2.45	0.21	0.52	0.19	0.60

Fig. 5 Mn_xO_y-rich precipitate formation from spiking of filtrate from corroded unit into control filtrate.

The spontaneous precipitate is high in manganese, and can be forced to occur in normally non-precipitating filtrates. Figure 5 illustrates the formation of manganese oxide-rich precipitates after spiking non-corroding Control filtrate with 5% to 50% volume (increasing concentration left to right in 5% increments) filtrate from the unit experiencing aggressive corrosion.

The following were noted as a result of the spiking studies:

(1) The reaction which causes Mn_xO_y to precipitate is accompanied by a reduction in pH, and an increase in ORP, as shown in Figures 6 and 7.

(2) Very little of the active ingredient in the filtrate from the corroded unit is required to cause Mn_xO_y precipitation to occur.

(3) The active agent in the filtrate from the corroded unit is very stable (i.e., still present after sitting over one year in the laboratory at room temperature).

Electrochemical Evaluations

The purpose of the first electrochemical test series was threefold – first, to determine if manganese would precipitate at a potential comparable to the high ORPs that were observed; second, to determine the effect of precipitated manganese on the electrochemical behavior (corrosion) of 2205 duplex stainless steel; and third, to determine the correlation between solution ORP and Alloy 2205. The test solutions were at a pH of 5.5 and contained 10,000 ppm chloride, 500 ppm maximum fluoride, and 0 or 500 ppm manganese. In the last test group, the oxidizer peroxymonosulfate (HSO_5) was incrementally added up to concentrations of either 111 ppm or 2000 ppm. Testing revealed the following:

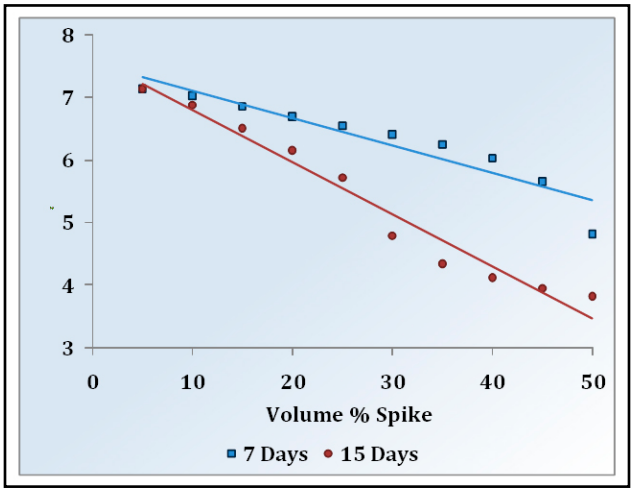

Fig. 6 pH versus Volume Percent of Spike.

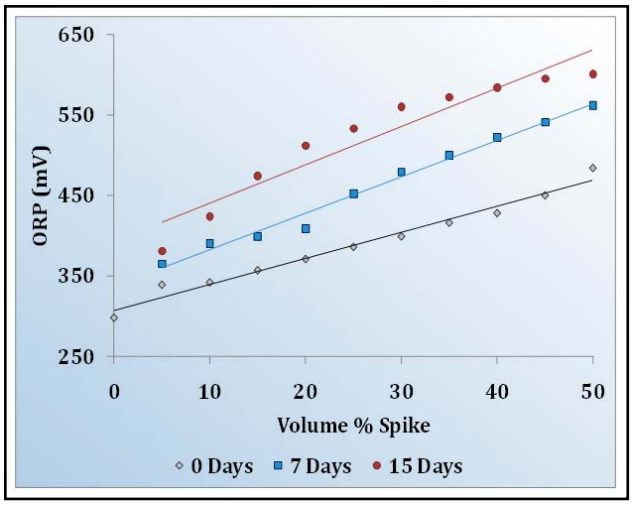

Fig. 7 ORP versus volume percent of spike.

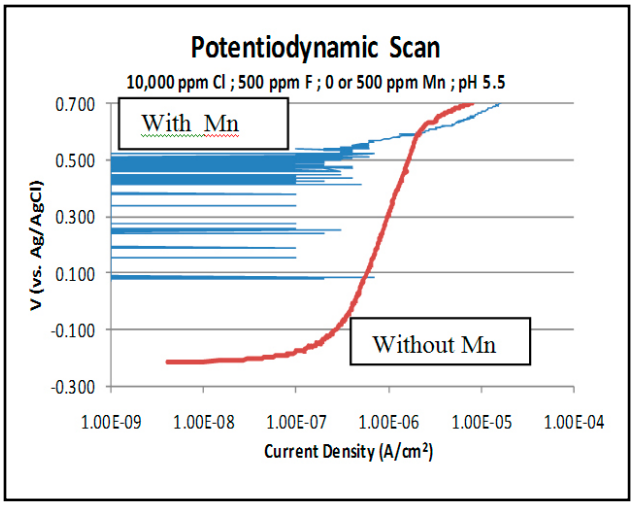

Fig. 9 PDS with and without manganese.

(1) The open circuit potential (OCP) was more anodic (positive) and less stable in the manganese-containing solution (refer to Figure 8). OCP is a measurement of the electrochemical potential of a metal.

(2) In manganese-containing solutions, the potentiodynamic scans (PDS) were very unstable (refer to Figure 9). A black precipitate (MnO_2) formed on the Alloy 2205 specimen at a potential comparable to the high ORPs that were observed in operating units.

(3) Electrochemically deposited MnO_2 increased the OCP of Alloy 2205 by approximately 0.3V (refer to Figure 10). At higher anodic potential, Mn appears to accelerate crevice attack.

(4) An oxidizer such as HSO_5 will cause precipitation of MnO_2. In the solutions containing HSO_5, MnO_2 precipitation occurred at approximately 0.5 V vs. Ag/AgCl reference electrode, which agrees with data from the Pourbaix Diagram for a manganese/water system.[2]

(5) HSO_5 additions to a solution containing no Mn caused a drastic increase in the ORP of the solution, but little increase in the OCP of the Alloy 2205. HSO_5 additions to a solution containing 500 ppm Mn caused a moderate increase in the ORP of the solution, but also caused a significant increase in the OCP of the Alloy 2205 (refer to Figure 11). The OCP increase in Mn-containing solutions appears to be due to the precipitation of MnO_2 as the HSO_5 was added.

In searching for a suspected oxidizing agent, titration of wet FGD filtrate samples from four aggressively corroding units, and eight units having no Mn_xO_y scale on the reaction tank surfaces, showed a significant difference in peroxodisulfate ($S_2O_8^{-2}$) concentration, specifically 1570 to 1680 ppm for the filtrates from the corroding units, compared to 227 ppm maximum for those units having no Mn_xO_y scale. According to Guberlet, peroxodisulfate can be formed by the following reactions, where M denotes a transition metal:[3]

(1) $M^{+3} + SO_3^{-2} \rightarrow M^{+2} + SO_3^{\bullet-}$

(2) $SO_3^{\bullet-} + O_2 \rightarrow SO_5^{\bullet-}$

(3) $SO_3^{\bullet-} + SO_5^{\bullet-} \rightarrow S_2O_8^{-2}$

Further, peroxodisulfate can react with available chloride ions in the absorber reaction tank slurry, resulting in the lowering of pH and the formation of chlorine gas. In aqueous solution, chlorine will readily react with water to form hypochlorite ion (ClO^-). A "swimming pool" odor is apparent at some plant sites and is falsely thought to elevate

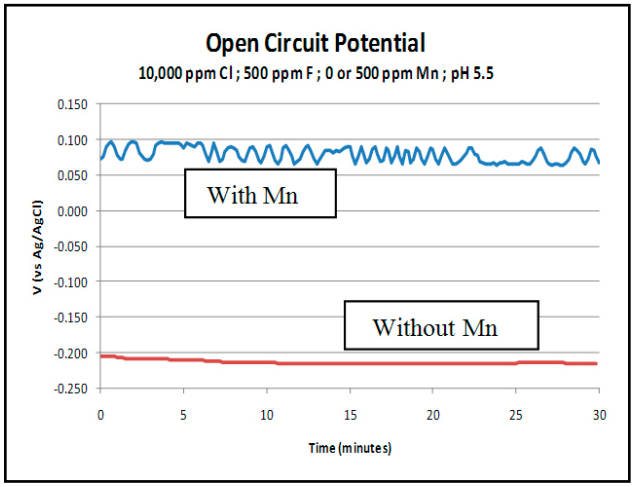

Fig. 8 OCP with and without manganese.

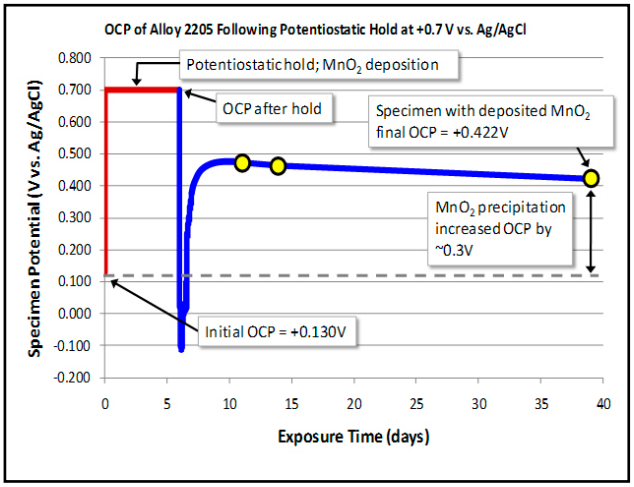

Fig. 10 Open circuit potential of Alloy 2205.

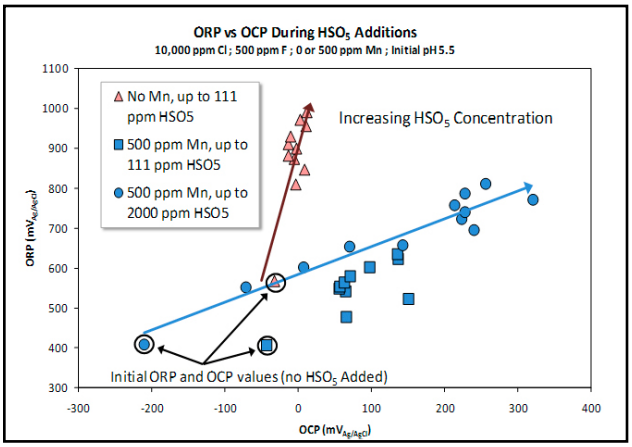

Fig. 11 ORP vs. OCP of Alloy 2205.

the level of acid gas detected at the stack. The lower pH may not be directly apparent within the absorber, masked by a higher reagent feed, but could be detected in bleed streams from which the solids have been removed.

(4) $S_2O_8^{-2} + 2Cl^- + 2Ca^{+2} \rightarrow 2CaSO_4 + Cl_2$

(5) $Cl_2 + H_2O^- \rightarrow 2H^+ + Cl^- + ClO^-$

According to Lutey and Richardson, MnO_2 deposits that physically contact metal surfaces, no matter how it occurs, serve as a galvanic cathode to promote corrosion of the metal.[1] As regards the unexpected corrosion mechanism in wet FGD reaction tanks, B&W PGG's current working hypothesis is:

$S_2O_8^{-2}$ formation → oxidation of manganese → Mn_xO_y precipitation and deposition on the alloy → galvanic cell formation → aggressive corrosion of alloy

Factors that influence the formation of peroxodisulfate include: the kinetic rate at which sulfite is oxidized to sulfate, oxidation air and mixing, and the relationship between sulfur-nitrogen chemistry and sulfur-oxygen chemistry. While peroxodisulfate routinely forms in wet FGD absorber slurries, a faster kinetic rate of oxidation is reasoned to lead to higher levels of $S_2O_8^{-2}$. As this oxidation is thought to be catalyzed by transition metals, a higher prevalence of transition metals in solution could also increase the rate of reaction. Higher amounts of transition metals may also increase the rate of formation of peroxodisulfate by providing more Mn^{+3} and Fe^{+3} for the initiation step of the free radical mechanism. Decreasing the amount of oxidation air entering the reaction tank, or introducing a reducing agent into the tank, should decrease the ORP of the slurry and the kinetic rate of peroxodisulfate formation. However, the oxidation state often controls solubility, and ORP will impact phase partitioning of many species as shown in Table 2, so the best compromise would be an intermediate ORP range where mercury is soluble, selenium is precipitated, and manganese is soluble.

Table 2
ORP Impacts on Phase Partitioning of Different Species

ORP	Mercury	Selenium	Manganese
High	Hg^{+2} Soluble	Se^{+6} Soluble	Mn^{+4} ↓ Precipitate
Medium	Hg^{+2} Soluble	Se^{+4} ↓ Precipitate	Mn^{+2} Soluble
Low	Hg^0 ↑ Vaporous	Se^{+4} ↓ Precipitate	Mn^{+2} Soluble

Sulfur-nitrogen chemistry may also play a role in peroxodisulfate formation, mainly through side reactions that may alter the kinetics of sulfite oxidation. A portion of the nitrogen dioxide [NO_2 (g)] in the flue gas can be absorbed into the absorber reaction tank slurry. NO_2 (g) absorption with oxygen results in aqueous sulfite oxidation.[4] Also, NO_2 (g) can react with sulfite to form a series of nitrogen-sulfur compounds, i.e., hydroxyl- amine disulfonic acid (HADS). The absorbed NO_2 (g) forms nitrite anion (NO_2^{1-}) in the aqueous phase of the reaction tank slurry, where it will eventually be oxidized to the nitrate anion (NO_3^{1-}). HADS may be limiting the chain reaction ($S_2O_8^{-2}$ formation) from happening, perhaps by chelating the manganese or by reducing it directly. HADS may be stopping the Mn in solution from going back and forth between its +2 and +3 oxidation states.

(6) $Mn^{+3} + HADS \rightarrow Mn^{+2} + H^+ + ON(SO_3^{-2})_2$

Microbiologically Influenced Corrosion

High manganese, black/purple scale with corrosion is well documented in literature as microbiologically influenced corrosion (MIC). To determine if MIC was the source of the aggressive corrosion, wet FGD absorber reaction tanks with different degrees of corrosion were sampled, as were tanks with no observed corrosion. Deoxyribonucleic acid (DNA) analyses were run on the slurry samples taken, and it was found that all the samples have similar microbial communities. Therefore, MIC is not considered to be the probable cause of aggressive corrosion or oxidizer formation.

Reaction Tank – Less Aggressive Corrosion

A less severe localized etching corrosion (refer to Figure 12), consistent with an under-deposit corrosion mechanism, has been observed in a number of Alloy 2205 absorber reaction tanks that were not experiencing the degree of corrosion associated with Mn_xO_y precipitation. This corrosion may also manifest as generalized pitting and/or oxide patinas, dependent upon the deposit composition and degree of deposit adherence. On a number of absorber reaction tanks showing no visible corrosion, random x-rays of the shell revealed sub-surface corrosion parallel to and perpendicular to the weld that appeared to initiate along the weld zone (refer to Figure13).

Analysis of scale shows that it is predominantly gypsum, with a much higher fluoride concentration at the scale-alloy interface than elsewhere in the scale. It should be noted that the Alloy 625 filler metal is not being attacked, and that this type of corrosion and x-ray indications are not being found on absorber surfaces above the reaction tank liquid level.

Electrochemical Testing

The objective of the laboratory electrochemical tests was to reproduce the corrosive attack observed in the Alloy 2205 reaction tanks. Test solutions were maintained at 130°F (54.4°C) at high potential for 34 days exposure with alloy specimens covered with different deposits added as sludge. Solutions 1 and 2 both contained 10,000 ppm chloride (as

Fig. 12 Visible localized under-deposit corrosion.

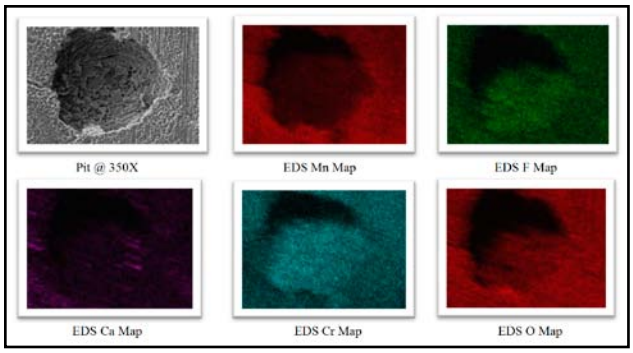

Fig. 14 SEM/EDS constituent mapping of solution 2 pit.

NaCl), 500 ppm fluoride (as NaF), with the deposit being CaF_2 (~100 grams). The deposit in Solution 2 was a combination of CaF_2 (~100 grams) and MnO_2 (~300 grams). Intial pH of the solutions was 5.5. Test analyses included energy dispersive x-ray spectroscopy (EDS) mapping of the alloy specimens' surfaces. Observations from this test series were:

1. Alloy 2205 specimens immersed in CaF_2 exhibited localized breakdown of the protective oxide, whereas the specimens immersed in CaF_2 and MnO_2 were noticeably pitted.
2. No manganese was found in the pits (refer to Figure 14). Consistent with Lutey and Richardson[1] the manganese appears to be acting as an accelerant to the pitting mechanism, but not a reactant in the pit itself.
3. All pits contained some level of fluoride inside the pit (refer to Figure 14), but not necessarily associated with calcium.

No manganese in the pits, along with fluoride in the pits not associated with calcium, indicates that the fluoride in the pits is a result of chemical reactions, and not the original CaF_2 added. Therefore, it can be concluded that fluoride played a significant role in the breakdown of the oxide and pitting on these specimens.

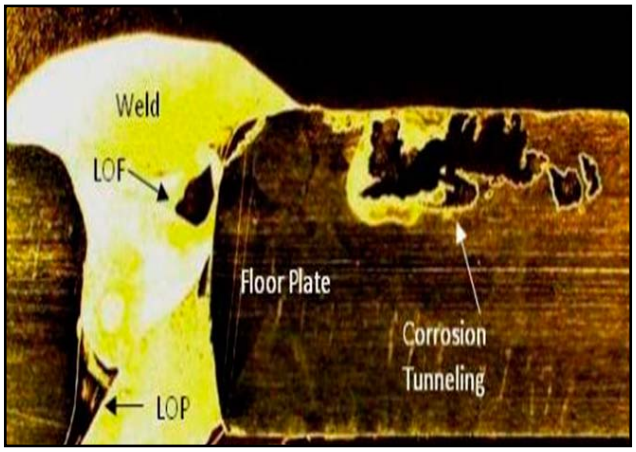

Fig. 13 Perpendicular-to-weld sub-surface corrosion.

For the second test series, Solution 1 was unchanged except that sparging with either air or nitrogen was added. Testing included incremental additions to Solution 1 of Mn^{+2} as $MnSO_4$ for Tests 1 and 2, Fe^{+3} as $Fe_2(SO_4)_3$ for Tests 3 and 4, Fe^{+2} as $FeSO_4$ for Tests 5 and 6, Ca^{+2} as $CaCl_2$ for Tests 7 and 8, and Mg^{+2} as $MgSO_4$ for Tests 9 and 10. The odd numbered tests were air sparged, while the even numbered ones were nitrogen sparged. Observations from this test series included:

1. Test 1 and 2 indicate that manganese, while it is maintained in solution, plays a small role in the corrosion process. The same can be said for calcium and magnesium ions in solution.
2. Fe^{+3} does play a role in the crevice corrosion of Alloy 2205 in a chloride and fluoride environment as evidenced by corrosion in the area of the lead wire with the overnight exposure. This is not a surprise in that Fe^{+3} ions are known oxidizers of stainless steels, which is the reason they are used in the ASTM A923 detrimental intermetallic phase detection tests and the ASTM G48 pitting and crevice corrosion resistance tests.
3. The Fe^{+3}/Fe^{+2} ratio plays a role in the crevice corrosion of Alloy 2205 in a chloride and fluoride environment as evidenced by a 300mV shift in OCP with the addition of Fe^{+3}.

A third series of electrochemical tests were run to determine if soluble fluoride was needed to cause pitting of anodically polarized Alloy 2205. The base solution had an inital pH of 5.5, contained 10,000 ppm chlorides (as NaCl), was air sparged, and the specimens immersed in CaF_2+MnO_2 deposits. Testing was performed with 0 and 500 ppm fluoride, with and without applied potential. Test results confirmed that corrosive attack was observed only with fluoride present, even at an applied potential of 100mV above OCP.

Regarding this less aggressive corrosion mechanism in wet FGD reaction tanks, B&W PGG's current working hypothesis is:

Deposition occurs

↓

Corrosion under the deposit initiates

↓

Following classical under-deposit/crevice corrosion theory,[5,6] the environment under the deposit becomes cation rich

↓

Fluoride ions, due to their smaller size and higher electronegativity, preferentially migrate to the metal surface to balance the charge, resulting in a concentrating mechanism for fluoride

↓

Fluoride reacts either with the alloy to accelerate the corrosion process, or reacts with calcium near the alloy surface to form CaF_2

↓

Following classical under-deposit/crevice corrosion theory, the pH near the metal surface is reduced due to hydrolysis of the metal fluoride[5,6]

↓

Inner layer with CaF_2 consolidates with time. $CaSO_4$ crystal growth occurs from this relatively dense inner layer

↓

On the active metal under the reduced pH conditions, fluoride can dissolve from the CaF_2 to accelerate the corrosion process. The rate of diffusion of fluoride to alloy surface equals the rate of reaction with the alloy.

Screening Test Development

The recent spate of absorber reaction tank corrosion has shown that the typical test methods, based on chloride and pH matrices, are inadequate for evaluation of alloy performance in the absorber reacion tank, because they do not address the chemistry associated with deposits. To better characterize the corrosion performance of alloys in wet FGD absorber reaction tanks, B&W PGG is using laboratory electrochemical testing (slow rate anodic scans and cyclic potentiodynamic scans) and immersion tests in a variety of conditions, followed by scanning electron microscope (SEM) and EDS evaluations.

All corrosion is an electrochemical process of oxidation and reduction reactions. As corrosion occurs, electrons are released by the metal (oxidation) and gained by elements (reduction) in the solution. Because there is a flow of electrons (current) in the corrosion reaction, it can be measured and controlled electronically. Therefore, controlled electrochemical experimental methods can be used to characterize the corrosion properties of alloys in solutions.

After numerous experiments in which the test solution constituents were varied to achieve/duplicate the corrosion observed in the absorber reaction tanks, the base solution selected contains 10,000 ppm chlorides (as NaCl), is air sparged, and maintained at 130°F (54.4°C). To best represent under-deposit chemistry of concentrated halogens, and low but stable pH, the solution contains 500 ppm fluoride (as NaF), and the initial pH is set at 3.5 by 0.1N H_2SO_4 addition. Testing begins only after a 14-hour soak to ensure a stable OCP starting point. A slow anodic scan rate of 0.025 mV/sec is used, while the cyclic polarization scan rate is 0.1667 mV/sec. Testing can be done with the base solution alone, or with the addition of either $CaSO_4$ or MnO_2 deposits.

As an example, the slow rate anodic scans (SRAs) for Alloy 2205 and Alloy 625 in $CaSO_4$ deposits are shown in Figure 15. The Alloy 2205 sample exhibited pitting/wastage corrosion, while the Alloy 625 sample exhibiting some staining but no pitting.

Results from the Alloys 2205 and 625 SRA evaluation include:

1. Presence of $CaSO_4$ deposits significantly increase the OCP of Alloy 2205, while the OCP of Alloy 625 is essentially unaffected by the deposits.
2. At the pitting potential, 2205 exhibits a 1000-fold instantaneous increase in current density. The higher the current density, the greater the corrosion.
3. As reported previously in other test results, EDS indicates that during the corrosion process fluoride is incorporated onto the 2205 surface, but not onto the Alloy 625 surface.
4. From further testing, it was found that:
   - The presence of $CaSO_4$ or MnO_2 deposits appear to have an effect on the corrosion response of Alloy 625, but does not lead to pitting.
   - The presence of $CaSO_4$ or MnO_2 deposits affects the corrosion response of the Alloy 2205 at all pH conditions tested, leading to pitting at potentials at or above 500 mV versus the Ag/AgCl reference electrode.
   - In the presence of deposits, corrosion behavior of Alloy 2205 is not a strong function of initial pH.

Figures 16 and 17 are the cyclic potentiodynamic scans (CPS) for Alloys 2205 and 625 respectively, with no deposits present. Note that there is a large hysteresis loop on the 2205 CPS (Figure 16) while the CPS for the 625 has essentially no hysteresis loop. The presence of a large hysteresis loop

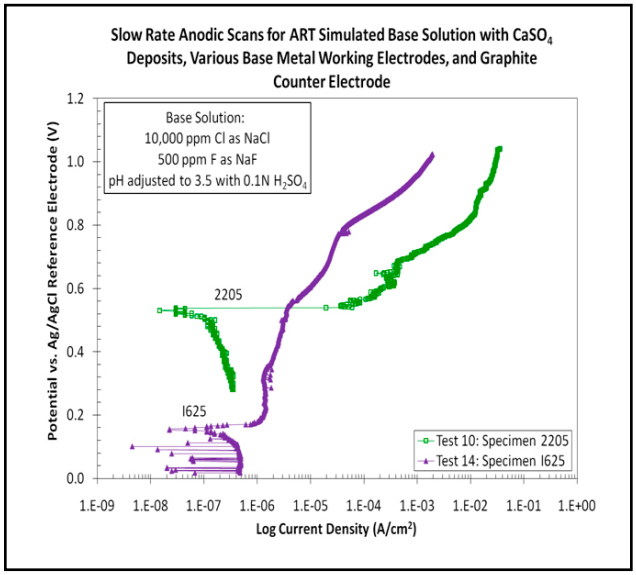

Fig. 15 Slow rate anodic scans.

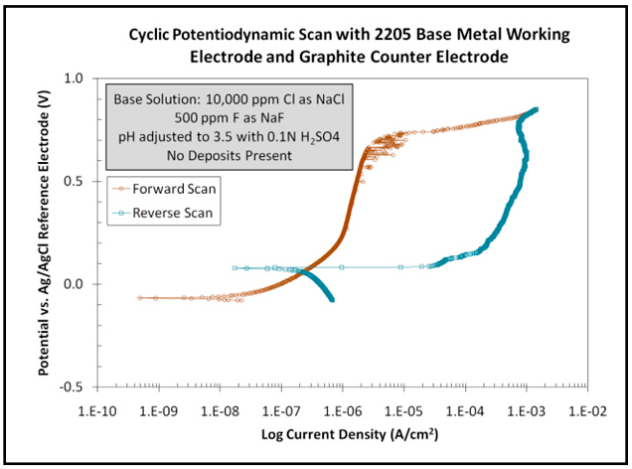

Fig. 16 Alloy 2205 cyclic scan.

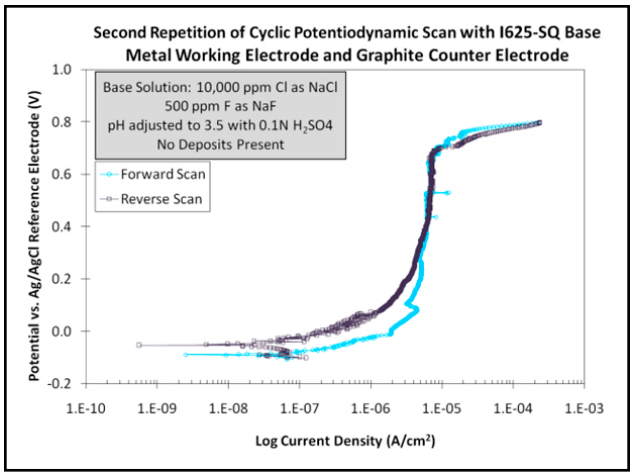

Fig. 17 Alloy 625 cyclic scan.

in a CPS is an indication that the test material is susceptible to pitting in the environment tested.[7,8] The absence of a hysteresis loop is an indication that the test material is resistant to pitting corrosion in the environment tested.[7,8]

In addition to Alloys 2205 and 625, nine other alloys have been tested, identified below by Pitting Resistance Equivalency numbers (PREn). PREn was calculated as (% Cr) + (3.3)(% Mo) + (16)(%N). Note that the minimum PREn values for Alloys 2205 and 625 are 34.4 and 46.4 respectively.

- Alloy A, an austenitic stainless steel with a minimum PREn of 31.8
- Alloy B, another duplex stainless steel with a minimum PREn of 35.2
- Alloy C, a 4.5% Moly stainless steel with a minimum PREn of 45.25
- Alloy D, a 6% Moly stainless steel with a minimum PREn of 41.2
- Alloy E, a 6% Moly stainless steel with a minimum PREn of 42.7
- Alloy F, a 6% Moly stainless steel with a minimum PREn of 50.2
- Alloy G, a 7% Moly stainless steel with a minimum PREn of 46.75
- Alloy H, a high Chromium, medium Nickel alloy with a minimum PREn of 48.2
- Alloy I, a high Nickel alloy having a minimum PREn of 64.0

All the alloys contained nitrogen, except for Alloy 625 and Alloy I.

In evaluating the alloys, the following factors were rated:

- Shape of the slow rate anodic (SRA) scan
- Elevation of the open circuit potential on the SRA scan
- Amount of pitting shown on the SEM
- Presence of fluorine and oxygen as shown on the EDS maps
- Shape of the cyclic potentiodynamic scan curves
- Reproducibility of the cyclic potentiodynamic scans

For alloy recommendations against fluoride-induced under-deposit corrosion in wet FGD reaction tanks, B&W PGG's testing to date indicates that there should be minimal to no corrosion concerns using either Alloy 625, Alloy E, Alloy F, or Alloy I. Two other alloys come very close in the ratings to the four recommended. The other five alloys fell far short in the ratings and would not be recommended. It should be noted that one 6% Moly and the 7% Moly alloy are not recommended – further investigation is necessary to determine the causes for the shortcomings of these two specific products.

Summary

The primary cause of corrosion in Alloy 2205 absorber reaction tanks appears to be fluoride-induced under-deposit attack. Fluoride diffuses through the deposit driven by the need for electroneutrality, concentrates, then reacts with the alloy to accelerate the corrosion process.

To characterize the corrosion performance of alloys in wet FGD absorber reaction tanks more effectively, B&W PGG is using slow rate anodic scans and cyclic potentiodynamic scans, in association with SEM and EDS mapping. To date, nine alloys have been evaluated. In addition to Alloy 625, three other alloys have been rated as being resistant to fluoride-induced under-deposit corrrosion in wet FGD reaction tanks.

Highly oxidative environments within some absorbers cause manganese in the slurry to precipitate as an oxide. The galvanic effect of these manganese oxide precipitates greatly exacerbates the under-deposit attack mechanism. Higher concentrations of the oxidizer peroxodisulfate have been found in absorber slurries of aggressively corroding reaction tanks. While peroxodisulfate routinely forms in wet FGD absorber slurries, it is reasoned that a faster kinetic rate of oxidation leads to higher levels of peroxodisulfate. While monitoring to ensure that full oxidation is not lost, decreasing the amount of oxidation air entering the reaction tank, or

introducing a reducing agent into the tank, should decrease the oxidation reduction potential of the slurry, reducing the kinetic rate of peroxodisulfate formation. However, the oxidation state often controls solubility, and oxidation reduction potential will impact phase partitioning of other species such as mercury and selenium.

References

1. Lutey, R. W. and Richardson, G.M., "Procedure Used for Root Cause Analysis: Pitting in Stainless Steel Tubes Associated with MnO_2 Deposition," *Corrosion*, San Diego, 2002, Paper 02472.
2. Pourbaix, M. *Atlas of Electrochemical Equilibria in Aqueous Solutions*, Volume 1, 1966, Pergamon Press.
3. Guberlet, Heinz, "Flue Gas Cleaning Chemistry," Power Plant Chemical Technology, International Conference., Kolding, Denmark, 1996.
4. Shen, C. H., Rochelle, G. T., "Nitrogen Dioxide Absorption and Sulfite Oxidation in Aqueous Sulfite," Environmental Science Technology, 1998, 32, 1994-2003.
5. Fontana, M.G. and Greene, N.D., *Corrosion Engineering*, Second Edition, McGraw-Hill, New York, New York, 1967, pp 41-44.
6. Uhlig, H.H., *Corrosion and Corrosion Control*, John Wiley & Sons, New York, New York, 1963, pp.272-274.
7. Annual Book of ASTM Standards, Section 3 Volume 3.02, "Wear and Erosion; Metal Corrosion," American Society for Testing and Materials, Philadelphia, Pennsylvania, 1996, ASTM G-61.
8. ASM Handbook, Volume 13A, "Corrosion: Fundamentals, Testing, and Protection", ASM Materials Park, Ohio, 2003, pp. 457 – 462.

Key words

Absorber, Alloy 2205, corrosion, crevice corrosion, cyclic potentiodynamic scan (CPS), energy dispersive x-ray spectroscopy (EDS), fluorine, fluoride-induced under-deposit corrosion, galvanic cell formation, hydroxyl-amine disulfonic acid (HADS), hysteresis loop, manganese, manganese oxide, mercury, microbiologically influenced corrosion (MIC), open circuit potential (OCP), oxidation reduction potential (ORP), peroxodisulfate, peroxymonosulfate, pitting resistance equivalency number (PREn), potentiodynamic scans, reaction tank, scanning electron microscope (SEM), selenium, slow rate anodic scan, sub-surface pitting, wet flue gas desulfurization, wet FGD